

APPLICATION OF SIMULATIONS TO THERMODYNAMIC PROPERTIES OF MATERIALS FOR MAGNETIC REFRIGERATION

A calorimetric approach to material's magnetocaloric parameters

J. F. Beltran-Lopez¹, M. Sazatornil¹, E. Palacios¹, R. Burriel¹

Received: date / Accepted: date

Abstract A magnetic refrigeration system is a complex system that involves the magnetocaloric effect (MCE) and the heat transfer problems working in a coupled manner. For this purpose, characterization of materials showing MCE is needed. Calorimetric characterization allows the obtention of thermodynamic variables needed for a precise quantification of this effect. More specifically, in systems with continuous magnetic field variation, in order to calculate the heat generation due to MCE, the knowledge of their magnetocaloric parameters - adiabatic temperature change ΔT_S and isothermal entropy change ΔS_T - and the heat capacity C_p , for every temperature and magnetic field present is needed. In this work, $\text{La}(\text{Fe}_{1-x-y}\text{Co}_x\text{Si}_y)_{13}$ family materials have been either characterized or interpolated, and used in numerical simulations in Comsol MultiphysicsTM software. The characterization was carried out with measurements of ΔT_S , ΔS_T and C_p and the calculation of other derived parameters, at different temperatures and magnetic fields.

Keywords Magnetocaloric effect · Direct measurements · Calorimetry · Simulation · Magnetic refrigeration

1 Introduction

Magnetic refrigeration is based on a reversible heating and cooling phenomenon given in certain magnetic materials, known as the magnetocaloric effect (MCE), as a result of

applying or removing an external magnetic field near their magnetic ordering transition temperature.

In order to achieve a higher efficiency, materials showing giant magnetocaloric effect (GMCE) as a result of an additional simultaneous transition, are often preferred for practical room temperature applications. Also, a lack of hysteresis in the transition is desirable to obtain a good efficiency. This technology is an alternative to actual compression-expansion systems and provides a high thermodynamic efficiency, which has been claimed to be able to reach up to 75% of Carnot's limit [1] compared to less than 40% of conventional systems (gas compression and expansion based), and uses no gases, showing therefore no direct greenhouse effect impact.

$\text{La}(\text{Fe}_{1-x-y}\text{Co}_x\text{Si}_y)_{13}$ family materials show GMCE, tunable transition temperatures, which can be set around room temperatures, and very little hysteresis, turning them into useful candidates for practical room temperature applications. The transition temperature is tuned by changing the cobalt content: the transition temperature increases and the first order character of the transition decreases as the cobalt content increases [2].

The heart of a magnetic refrigeration system is what is called the active magnetic regenerator (AMR), in which the magnetocaloric material (MCM) is placed. The AMR allows the obtention of temperature spans much larger than just the ΔT_S produced by a single field change, making it work as active MCM and as regenerator simultaneously. The concept and theory of an AMR can be found in [3] and [4], respectively. The heat transfer mechanism from the cold sink to the regenerator and from there to the hot sink is an important limitation for the commercialization of this technology, since it entails an important efficiency practical limitation. The development and improvement of the heat transfer system that allows the practical use of the MCE and the search for new materials showing GMCE are within the main concerns in the development of this technology.

¹ J. F. Beltran – Lopez
Instituto de Ciencia de Materiales de Aragón (ICMA) and
Departamento de Física de la Materia Condensada.
CSIC – University of Zaragoza.
Pedro Cerbuna 12, 50009 Zaragoza, Spain.
Tel. : +34 – 976762649
E – mail : jebelt@unizar.es

The temperature changes that can be obtained with the simple application of magnetic field are quite small for any practical application in cooling systems. A very strong magnetic field would be necessary to produce a relevant temperature change. Field values obtained with affordable permanent magnets, between 1 and 2 T, turn out into temperature changes below 5 degrees. However, using an AMR with several graded materials of different transition temperatures (Figure 1), the temperature span obtained can be enlarged much over the change obtained with a single field change and, at the same time, the refrigeration power is substantially increased compared to using a single MCM [5], allowing a wide working temperature window defined by the combination of the peaks' widths of the MCMs used in the AMR.

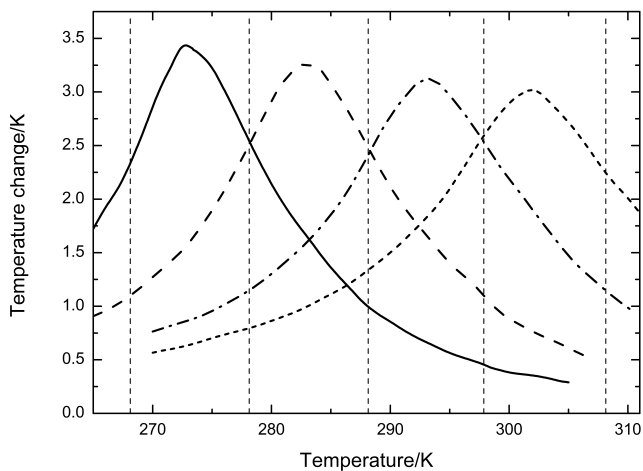


Fig. 1 Graphs of the ΔT_S of four interpolated $\text{La}(\text{Fe}_{1-x-y}\text{Co}_x\text{Si}_y)_{13}$ materials in an AMR, for field increases of 1.6 T. The vertical dashed lines depict the temperature range in which each material is used in a supposed multimeral AMR.

The study of the heat transfer mechanisms involved in the performance of a magnetic refrigerator is of great importance to determine the suitability of its design. Numerical simulations are a very useful tool to understand the heat transfer mechanisms and the implication of the different design parameters in the system's performance. Calorimetric characterization of materials showing MCE or GMCE is necessary in order to evaluate them and provide accurate data for systems simulation.

The thermomagnetic characterization of materials of the $\text{La}(\text{Fe}_{1-x-y}\text{Co}_x\text{Si}_y)_{13}$ family was carried out with experimental measurements and, in some cases, using a material's properties interpolation method that we have developed. The samples were provided by the company Vacuumschmelze GmbH. These materials have a well established manufacturing process and these samples with different stoichiometries are being used in several laboratories. The materials, prepared at a preindustrial level, have shown consistent results

Table 1 Approximate stoichiometries of the measured compounds.

MPS1175	$\text{La}(\text{Fe}_{0.853}\text{Co}_{0.067}\text{Si}_{0.08})_{13}$
MPS1178	$\text{La}(\text{Fe}_{0.842}\text{Co}_{0.079}\text{Si}_{0.079})_{13}$
MPS1180	$\text{La}(\text{Fe}_{0.834}\text{Co}_{0.088}\text{Si}_{0.078})_{13}$

in their chemical analysis and magnetocaloric properties [2, 6]. The resulting thermomagnetic data have been introduced in a Comsol MultiphysicsTM model to simulate a magnetic refrigeration system.

2 Characterization of magnetocaloric materials

The measured materials are from $\text{La}(\text{Fe}_{1-x-y}\text{Co}_x\text{Si}_y)_{13}$ family, having different stoichiometries (Table 1) and, therefore, different transition temperatures.

The relevant thermodynamic parameters to characterize the MCE of a magnetic material are:

- ΔS_T : Entropy change of the sample when the magnetic field is increased isothermally.
- ΔT_S : Temperature change of the sample when the magnetic field is increased adiabatically.

We also obtain the specific heat of a sample at different magnetic fields with our adiabatic calorimeter, using either step C_p points or dynamic thermograms. The specific heat varies greatly and its curves are therefore needed to evaluate correctly the MCE of the material.

A summary of the most relevant parameters of the measured $\text{La}(\text{Fe}_{1-x-y}\text{Co}_x\text{Si}_y)_{13}$ materials is provided in tables 2 and 3.

2.1 Experimental set-up

The measurements required to determine the magnetocaloric parameters were made using our installation, which consists of an adiabatic system cooled by a cryocooler that can work as an adiabatic calorimeter or measure directly both magnetocaloric parameters [7]. The magnet used in our installation is a superconducting magnet providing fields up to 9 T. The working temperature of the adiabatic system goes from 1.5 K to 350 K.

2.2 Heat capacity measurements

There are two ways of obtaining the specific heat of a sample with our adiabatic calorimeter: step C_p points or dynamic thermograms.

A step C_p measurement involves the application of heat to the sample vessel while maintaining the adiabatic screen following the temperature of the vessel. C_p is computed as

Table 2 T_c and $C_p(T_c)$ of measured $\text{La}(\text{Fe}_{1-x-y}\text{Co}_x\text{Si}_y)_{13}$ compounds.

Variable	$\text{La}(\text{Fe}_{0.853}\text{Co}_{0.067}\text{Si}_{0.08})_{13}$	$\text{La}(\text{Fe}_{0.842}\text{Co}_{0.079}\text{Si}_{0.079})_{13}$	$\text{La}(\text{Fe}_{0.834}\text{Co}_{0.088}\text{Si}_{0.078})_{13}$
T_c (K)	277.5	295.7	307.0
C_p (J/(kg·K))	871.7	807.3	766.9

Table 3 Maximum values of $-\Delta S_T$ (J/(kg·K)) and ΔT_S (K) and their temperatures, for different field change values, of measured $\text{La}(\text{Fe}_{1-x-y}\text{Co}_x\text{Si}_y)_{13}$ compounds.

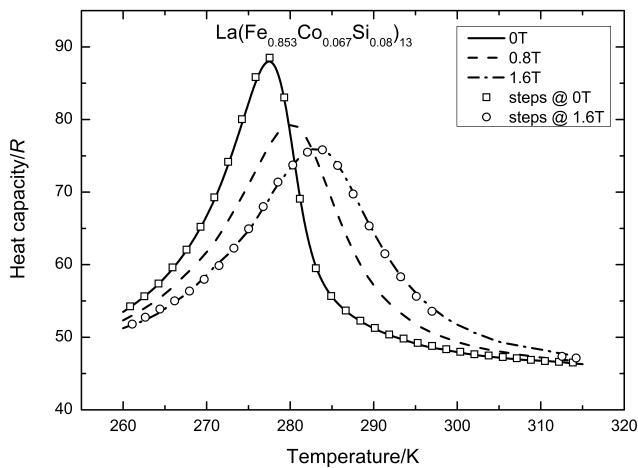
Field	$\text{La}(\text{Fe}_{0.853}\text{Co}_{0.067}\text{Si}_{0.08})_{13}$		$\text{La}(\text{Fe}_{0.842}\text{Co}_{0.079}\text{Si}_{0.079})_{13}$		$\text{La}(\text{Fe}_{0.834}\text{Co}_{0.088}\text{Si}_{0.078})_{13}$	
	T_{max}	$-\Delta S_{T,max}$	T_{max}	$-\Delta S_{T,max}$	T_{max}	$-\Delta S_{T,max}$
0.8 T	279.9	4.9	298.7	4.1	310.8	3.6
1.6 T	280.5	8.7	299.2	7.0	311.2	6.3
3 T	281.5	12.9	300.0	11.0	312.0	10.3
5 T	282.9	17.5	301.0	15.8	313.0	14.5

Field	$\text{La}(\text{Fe}_{0.853}\text{Co}_{0.067}\text{Si}_{0.08})_{13}$		$\text{La}(\text{Fe}_{0.842}\text{Co}_{0.079}\text{Si}_{0.079})_{13}$		$\text{La}(\text{Fe}_{0.834}\text{Co}_{0.088}\text{Si}_{0.078})_{13}$	
	T_{max}	$\Delta T_{S,max}$	T_{max}	$\Delta T_{S,max}$	T_{max}	$\Delta T_{S,max}$
0.8 T	280.1	1.8	298.6	1.7	311.5	1.6
1.6 T	280.4	3.3	298.9	3.0	311.6	2.9
3 T	281.0	5.3	299.3	5.0	312.1	4.9
5 T	281.8	7.9	300.0	7.6	312.7	7.2

the applied heat, Q , divided by ΔT , where ΔT is the temperature increment.

A thermogram consists on heating or cooling the vessel at a slow constant rate at around 1 mK/s and recording the temperature vs. time $T(t)$. This $T(t)$ curve is later converted to a $C_p(T)$ curve [7]. A temperature controller maintains a fixed temperature difference between an adiabatic screen and the internal vessel containing the sample. This turns into a heat gain or loss through conduction and radiation terms, from which we deduce the $C_p(T)$ curve.

An example of C_p measurements obtained for MPS1175 is shown in Figure 2.

**Fig. 2** Measured C_p/R curves for MPS1175 at three field values. The curves were obtained from thermograms, while the points marked with symbols were obtained from steps.

2.3 Measuring the magnetocaloric parameters

Isothermal entropy change: The ΔS_T measurements are performed differently depending on whether the material shows direct or inverse MCE. A material with direct MCE tends to cool when the magnetic field is removed. In order to perform this operation isothermally, heat must be applied to the vessel to keep the temperature constant. Hence, ΔS_T can be given as $-Q/T$, where Q is the heat applied during the process and T the constant temperature. When the material presents inverse MCE, the procedure is the opposite, the magnetic field is increased, and again heat must be applied to make the process isothermal. In this case, ΔS_T is expressed as $+Q/T$. This experimental method was described in [8].

Adiabatic temperature change: The procedure to measure ΔT_S is to change the magnetic field applied to the sample and measure the temperature increase, while maintaining adiabatic insulation [7]. The magnetic field is successively increased from 0 to 5 T in a succession of steps and then down to 0 T again.

Our results have been compared with literature values obtained in compounds of the same family at other fields [9]. The comparison of our values with other previously published results is not direct due to the lack of results given under the same conditions. Nevertheless, the regularity of the thermodynamic values along this family of compounds allows a comparison through a combined interpolation in field and in temperature. The comparison with values reported for three samples of the same family [9] showed differences lower than 5% for all the parameters C_p , ΔS_T and ΔT_S . This is a very good agreement, taking into account that we are

using the external field applied and not the resulting internal field in the samples, as the referred paper does.

3 Interpolation of materials' properties

We have found that, at least within the temperature range of interest, the $\text{La}(\text{Fe}_{1-x-y}\text{Co}_x\text{Si}_y)_{13}$ family of materials follows a corresponding states law, which allows the prediction of the materials' parameters of interest by interpolation. Using the data of two materials plus the temperature of the peak for the variable considered in a new material, we can obtain the whole plot of the variable for the new material. This means that we can approximate ΔT_S , ΔS_T and C_p just by knowing their peak temperatures. Also, peak temperatures at different magnetic field values can be approximated, given the measured values at different fields for several of these materials, with different transition temperatures. The interpolated curves match almost perfectly with the measured data (Figure 3).

Since we interpolate only the anomalies of the curves, in the case of C_p/R , the interpolation process must start with the subtraction of the base line, for which the C_p/R of $\text{LaFe}_{12}\text{Si}$, whose peak temperature lies below 200 K, was used, adjusting it by means of a Debye function plus a linear electronic contribution. Since the temperatures of interest are between 270 and 310 K, this can be approximated using a straight line (1).

$$\frac{C_p}{R} = 31.12 + 3.885 \times 10^{-2} \times T \quad (1)$$

After this, a normalization of the temperature is done for the reference materials:

$$x = \frac{T - T_0}{T_0} \quad (2)$$

where T_0 is the peak's temperature of the material and x is the normalized temperature. After a linear interpolation along the y-axis, the variable change is undone and, in the case of C_p/R , the base line is added to the results.

The values of ΔT_S , ΔS_T and C_p are later defined as double interpolation tables in B and T in the simulation model, which finally provide the value of these parameters at the field and temperature at which the material is subjected. The practical result is like having a set of response curves for every parameter as it is shown in Figure 4 as an example.

4 Obtaining derived materials' properties

The model to be simulated is based on a rotatory cylindrical double Halbach magnet system. It produces a field which

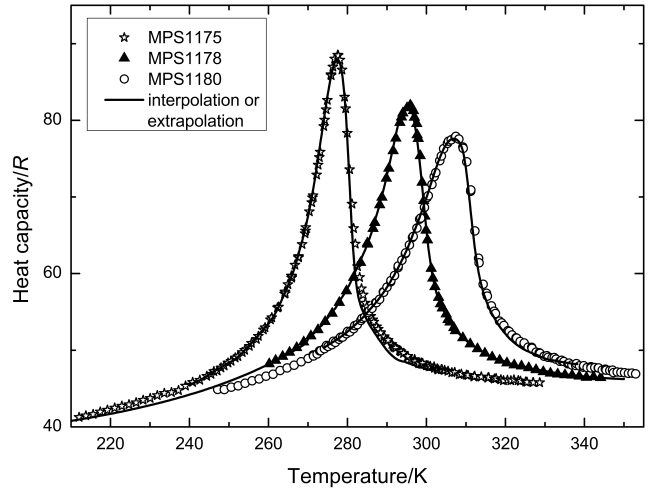


Fig. 3 Interpolation and extrapolation of C_p/R of three previously measured materials, starting from the data of the other two measured materials of the family. The interpolated or extrapolated curves are shown as solid lines and the measured data are shown with symbols.

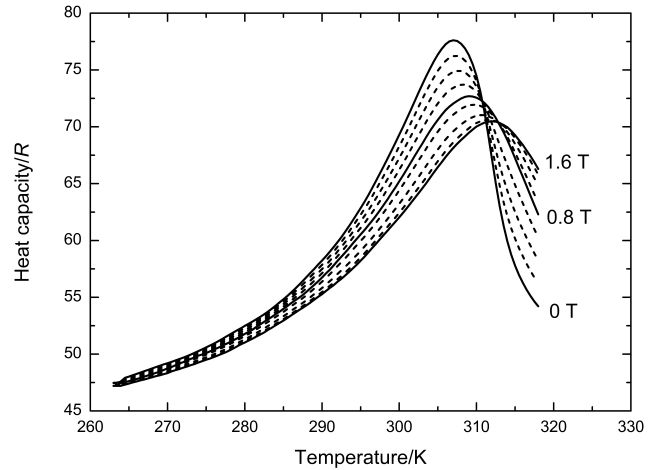


Fig. 4 Interpolation of C_p/R at different magnetic field values using the measurements at three fields, for the material MPS1180. Measured curves are solid, while dashed ones are interpolated. Starting from the right-bottom side, interpolated field values are: 0.2, 0.4, 0.6, 1, 1.3 and 1.5 T.

varies continuously from a minimum value (ideally 0 T) to a maximum value and back to the minimum value. The MCE power is calculated with the expression:

$$W_{MCE} = \rho \times C_p \times \frac{d(\Delta T_S)}{dB} \times \frac{d|B|}{dt} \quad (3)$$

where ρ is the density.

C_p depends on the temperature and the magnetic field, $d(\Delta T_S)/dB$ is a function that also depends on the temperature and the magnetic field and B depends on time and on the position within the magnets' assembly (ideally, the position along the longitudinal axis of the concentric magnets).

Using expression (3), the ΔS_T measurements are not necessary. However, they would be necessary if the applied mag-

netic field could be regarded as a stepping system, going instantaneously from minimum field to maximum field and viceversa.

A procedure has been developed in order to obtain the derivative $d(\Delta T_S)/dB$ for every field, starting from the measured ΔT_S data: First obtain a four point interpolation function for every temperature in the data set, $\Delta T_S = a_1 \times B + a_2 \times B^2$. Then, smooth out a_1 and a_2 (OriginPro™ smoothing tools were used for this purpose) and calculate the derivative analytically:

$$\frac{d(\Delta T_S)}{dB} = \tilde{a}_1 + \tilde{a}_2 \times B \quad (4)$$

The obtained set of functions (one for every temperature value in the data set) is used to obtain the values of the derivative at the temperatures and magnetic field values in the data set, forming a double interpolation table (magnetic field and temperature) which is later defined in Comsol Multiphysics™ as such.

C_p data are also turned into double interpolation tables and defined in the simulation software as well, while $d|B|/dt$ values are obtained by defining an analytical function in the model.

For the double Halbach assembly, if only the exterior magnet is rotating while the interior one is fixed, $d|B|/dt$ can be expressed with equation 5. If both magnets rotate, the derivative is given by equation 6.

$$\begin{cases} \frac{d|B|}{dt} = -\pi f B_{max} \sin(\pi f t); & (4n-1)\frac{\pi}{2} < \pi f t < (4n+1)\frac{\pi}{2} \\ \frac{d|B|}{dt} = \pi f B_{max} \sin(\pi f t); & (4n+1)\frac{\pi}{2} < \pi f t < (4n+3)\frac{\pi}{2} \end{cases} \quad (5)$$

$$\begin{cases} \frac{d|B|}{dt} = -2\pi f B_{max} \sin(2\pi f t); & (4n-1)\frac{\pi}{2} < 2\pi f t < (4n+1)\frac{\pi}{2} \\ \frac{d|B|}{dt} = 2\pi f B_{max} \sin(2\pi f t); & (4n+1)\frac{\pi}{2} < 2\pi f t < (4n+3)\frac{\pi}{2} \end{cases} \quad (6)$$

In both of the above equations 5 and 6, f is the rotation frequency, B_{max} is the maximum magnetic field and n is a non negative integer.

5 Conclusions

As a general conclusion from this MCE and calorimetric characterization we obtained very precise values for the relevant parameters, C_p , ΔS_T and ΔT_S , of some compounds of the $\text{La}(\text{Fe}_{1-x-y}\text{Co}_x\text{Si}_y)_{13}$ family, which are practical materials for cooling applications, around room temperature.

A method to obtain $d(\Delta T_S)/dB$ and a material interpolation procedure have been developed and applied to MCMs of the $\text{La}(\text{Fe}_{1-x-y}\text{Co}_x\text{Si}_y)_{13}$ family, in order to obtain the necessary data to carry out magnetic refrigeration simulations, without the need of measuring the ΔT_S , ΔS_T and C_p of all the materials used in the magnetic refrigerator model. The methodology also allows to approximate the temperature of the peaks of ΔT_S , ΔS_T or C_p of a given material of the family, just by knowing the temperature of one of them. This allows simulating combinations of $\text{La}(\text{Fe}_{1-x-y}\text{Co}_x\text{Si}_y)_{13}$ materials with different transition temperatures, even before they are available, in order to seek the optimum MCM combinations for a given cooling system.

Acknowledgements The authors acknowledge BSH Electrodomésticos España contract 2013/0011, the Spanish MINECO project MAT2013-44063R and DGA Consolidated Group E100.

References

- Petersen TF, Pryds N, Smith A, Hattel J, Schmidt H, Knudsen HH. Two-dimensional mathematical model of a reciprocating room-temperature active magnetic regenerator. *Int J Refrigeration*. 2008;31:432-443.
- Katter M, Zellmann V, Reppel GW, Uesteuner K. Magnetocaloric properties of $\text{La}(\text{Fe},\text{Co},\text{Si})_{13}$ bulk material prepared by powder metallurgy. *IEEE Trans Magn*. 2008;44(11):3044-3047.
- Steyert WA. Stirling cycle rotating magnetic refrigerators and heat engines for use near room temperature. *J Appl Phys*. 1978;49:1216-1226.
- Barclay, JA. The theory of an active magnetic regenerative refrigerator. *Proceedings of the Second Biennial Conference on Refrigeration for Cryocooler Sensors and Electronic Systems*. NASA Conference Publication 2287. 1983;375-387.
- Richard MA, Rowe AM, Chahine R. Magnetic refrigeration: Single and multimaterial active magnetic regenerator experiments. *J Appl Phys*. 2004;95:2146-2150.
- Liu J, Moore JD, Skokov KP, Krautz M, Löwe K, Barcza A, Katter M, Gutfleish O. Exploring $\text{La}(\text{Fe},\text{Co},\text{Si})_{13}$ -based magnetic refrigerants towards application. *Scripta Materialia*. 2012;67:584-589.
- Tocado L, Palacios E, Burriel R. Adiabatic measurement of the giant magnetocaloric effect in MnAs. *J Therm Anal Calorim*. 2006;84(1):213-217.
- Palacios E, Wang GF, Burriel R, Provenzano V, Shull RD. Direct measurement of the magnetocaloric effect in $\text{Gd}_5\text{Si}_2\text{Ge}_{1.9}\text{Ga}_{0.1}$. *J Phys: Conf Series*. 2010;200:092011(1-2).
- Bjørk R, Bahl CRH, Katter M. Magnetocaloric properties of $\text{LaFe}_{13-x-y}\text{Co}_x\text{Si}_y$ and commercial grade Gd. *J Magn Magn Mater*. 2010;322:3882-3888.